8512 *Biochemistry* **2010,** *49,* 8512–8519
DOI: 10.1021/bi1009908

BIOCHEMISTRY
including biophysical chemistry & molecular biology
Article

Synergistic and Inhibitory Effects of Aminopeptidase Peptides on *Bacillus thuringiensis* Cry11Ba Toxicity in the Mosquito *Anopheles gambiae*[†]

Rui Zhang,[‡] Gang Hua,[‡] Jeffrey L. Urbauer,[§] and Michael J. Adang*[,‡,§]

[‡]*Departments of Entomology and* [§]*Biochemistry and Molecular Biology, University of Georgia, Athens, Georgia 30602-2603*

Received June 18, 2010; Revised Manuscript Received August 26, 2010

ABSTRACT: Cry11Ba produced by *Bacillus thuringiensis* subsp. *jegathesan* is an active toxin for larvae of the mosquito *Anopheles gambiae*. A 106-kDa aminopeptidase N (APN), called AgAPN2, was previously identified as a Cry11Ba receptor in *A. gambiae*. A 70-kDa fragment of AgAPN2 expressed in *Escherichia coli* binds Cry11Ba with high affinity (K_d = 6.4 nM) and inhibits Cry11Ba activity by 98% in bioassays [Zhang et al. (2008) *Biochemistry 47*, 11263−11272]. To identify regions involved in toxicity, we truncated the 70-kDa APN fragment into peptides of 28- and 30-kDa ta and tb, respectively, and tested their abilities to mediate toxicity and bind Cry11Ba. While AgAPN2ta reduced Cry11Ba toxicity by 85%, AgAPN2tb showed a significant enhancement effect on Cry11Ba toxicity. The purified peptides showed evidence of structural folding and bound the same site(s) on Cry11Ba with high affinity. The inhibitory AgAPN2ta blocked Cry11Ba binding to brush border membrane vesicles (BBMV) of *A. gambiae* whereas the toxicity enhancing AgAPN2tb increased Cry11Ba binding on BBMV. A deletion at the N-terminus (^{336}S−P^{420}) of AgAPN2ta significantly reduced AgAPN2ta binding to Cry11Ba and its inhibitory effect. Deletion of the central region (^{676}I−W^{760}) of AgAPN2tb eliminated its increased toxin binding and toxicity enhancement effect without affecting Cry11Ba binding. A "bridge" model is proposed for AgAPN2tb action whereby the peptide binds Cry11Ba and vectors it to sites on the larval midgut.

The bacterium *Bacillus thuringiensis* subsp. *israelensis* (Bti)[1] has been used worldwide as an important mosquito control agent for decades (*1*). The active ingredient of Bti is a parasporal crystal complex composed of four Cry proteins (Cry4Aa, Cry4Ba, Cry10Aa, and Cry11Aa) and two cytolytic proteins (Cyt1Aa and Cyt2Ba) (*2*). Concerns about potential mosquito resistance development to Bti have led to discoveries of other mosquitocidal toxins with high potency. Cry11Ba produced by *Bacillus thuringiensis jegathesan* (Btjeg) is the single most effective toxin against mosquitoes to date. Cry11Ba shares 58% similarity to Cry11Aa and is 7−34-fold more toxic to mosquito larvae (*3*).

The resolved structures of Cry proteins show a conserved 3D topology, suggesting a common mode of action (*4*−*9*). Two models of the mechanism of toxicity are proposed (reviewed in ref *10*). The colloid-osmotic lysis model suggests that proteolytically activated toxins bind cadherin, oligomerize, and then bind glycosylphosphatidylinositol- (GPI-) anchored aminopeptidase (APN) and GPI-anchored alkaline phosphatase (ALP) to induce toxicity (*11*). An alternative model proposes the activation of intracellular signaling pathways by toxin monomer binding to cadherin without the need of the toxin oligomerization step to cause cell death (*12*). Whether toxicity is independent of toxin oligomerization remains arguable; however, the toxin−receptor interaction has been implicated in both models as the major determinant of toxin specificity.

APN has long been implicated as a Cry1 toxin binding protein in a number of lepidopteran species (reviewed in ref *10*). As a glycoprotein, APN interacts with Cry toxins through either glycan moieties or amino acid residues. For example, Cry1Ac has been shown to bind an *N*-acetylgalactosamine (GalNAc) moiety on APNs in the midgut of lepidopteran species [*Manduca sexta* (*13*), *Heliothis virescens* (*14*), and *Lymantria dispar* (*15*)]. In contrast, Cry1Aa and Cry1Ab are believed to bind APN only in a carbohydrate-independent manner (*16*, *17*). Yaoi et al. (*18*) localized a Cry1Aa binding site on *Bombyx mori* APN to the region between ^{135}Ile and ^{198}Pro. This region contains amino acid residues RXXFPXXDEP conserved among APNs from different species and thus has been suggested as a common Cry1Aa binding region (*16*, *19*). Recently, a 112-kDa APN (AaeAPN1) in the midgut of the mosquito *Aedes aegypti* was shown to bind Cry11Aa through the region between ^{525}Arg and ^{778}Leu (*20*). Unlike the Cry1Aa binding site near the N-terminus of the BmAPN, the Cry11Aa binding region was located to the C-terminal region of AaeAPN1. In our previous study, we identified a 106-kDa APN (AgAPN2) as a Cry11Ba binding protein and putative receptor in *Anopheles gambiae* (*21*). The 70-kDa partial AgAPN2 expressed in *Escherichia coli* binds Cry11Ba with high affinity and blocks Cry11Ba toxicity toward mosquito larvae. This APN fragment shows no similarities to the reported Cry1Aa and Cry11Aa binding regions. Collectively, the data provide evidence that a few primary amino acid sequences on APNs are probably key factors in determining toxin specificities.

[†]This research was supported by National Institutes of Health Grant R01 AI 29092 to D. H. Dean (The Ohio State University) and M.J.A.

*Address correspondence to this author at the Department of Entomology, University of Georgia. E-mail: adang@uga.edu. Phone: 706-542-2436. Fax: 706-542-2279.

[1]Abbreviations: ALP, alkaline phosphatase; APN, aminopeptidase N; Bti, *Bacillus thuringiensis* subsp. *israelensis*; Btjeg, *Bacillus thuringiensis jegathesan*; BSA, bovine serum albumin; BBMV, brush border membrane vesicle; CD, circular dichroism; CAPS, 3-(cyclohexylamino)propanesulfonic acid; GPI, glycosylphosphatidylinositol; PI-PLC, phosphatidylinositol-specific phospholipase C; PCR, polymerase chain reaction.

 Published on Web 09/01/2010

Table 1: Primers Used in This Study[a]

primer	primer sequence (5′−3′)
Primers for Cloning AgAPN2ta and AgAPN2tb	
AgAPN2ta-F	5′-GTCCCATATGTCCACCAGTATGCAACAG-3′
AgAPN2ta-R	5′-TACTCTCGAGCCACAGAATGGCATCGTAG-3′
AgAPN2tb-F	5′-CATTCATATGGGAAAAATCAGCAAGGCGC-3′
AgAPN2tb-R	5′-AGGCCTCGAGCACATTCGTGTAACTA-3′
Primers for Cloning AgAPN2ta Deletions	
AgAPN2ta-Del1	
AgAPN2ta/Del1-F	5′-GACTCATATGGTCTACACGCAAGCTCAGACCAG-3′
AgAPN2ta-R	5′-TACTCTCGAGCCACAGAATGGCATCGTAG-3′
AgAPN2ta-Del2	
AgAPN2ta/Del2-F	5′-GGTCGAATTCACCAGCCACGACACTGGATTCACC-3′
AgAPN2ta/Del2-R	5′-GCGTGAATTCGGGATGAGTCATAGGGTGGGTAG-3′
AgAPN2ta-Del3	
AgAPN2ta/Del3-F	5′-CATTGAATTCCTCGAGCACCACCACCACCACC-3′
AgAPN2ta/Del3-R	5′-CGTGGAATTCAACAGTGACCAGAGGATAGCCAGG-3′
Primers for Cloning AgAPN2tb Deletions	
AgAPN2tb-Del1	
AgAPN2tb/Del1-F	5′-TCGCCATATGCATGCTGATGATGAGAAGCTGTTC-3′
AgAPN2tb-R	5′-AGGCCTCGAGCACATTCGTGTAACTA-3′
AgAPN2tb-Del2	
AgAPN2tb/Del2-F	5′-GTTCAAGCTTAATCAATATCTGACAACGAACGTGGC-3′
AgAPN2tb/Del2-R	5′-TGGAAAGCTTGTCTAGGATGTGGGCCGTGAACA-3′
AgAPN2tb-Del3	
AgAPN2tb-F	5′-CATTCATATGGGAAAAATCAGCAAGGCGC-3′
AgAPN2tb/Del3-R	5′-GATACTCGAGCCACAAGAACTCGAACTCCTCCGT-3′

[a]Endonuclease sites are underlined.

To further characterize interactions between Cry11Ba and 70-kDa AgAPN2t, we divided the peptide into two fragments of similar size. We showed that one fragment inherited the inhibitory effect of the 70-kDa peptide. By using a combination of in-frame deletions and binding assays, we located a region (^{336}S−P^{420}) on AgAPN2 that is essential for toxin binding and blocking toxicity *in vivo*. Unexpectedly, we also observed an enhancing effect of another fragment (^{591}G−V^{843}) on Cry11Ba toxicity. Previously, an enhancing effect had been found with fragments of cadherin (*22*−*24*). Our finding of an enhancing role for a fragment of AgAPN2 is the first report that a non-cadherin fragment of a Cry toxin-binding protein can act as a synergist of Cry toxicity to pest insects.

EXPERIMENTAL PROCEDURES

Purification and Biotinylation of Cry11Ba Toxin. The Bt strain 407 (*3*) producing Cry11Ba protein was grown in complex sporulation medium (*21*) supplemented with erythromycin antibiotic. The spore crystal mixture was washed, crystals were separated on NaBr step gradients, and protoxin was prepared as previously described (*21*). Purified Cry11Ba crystals were washed twice with distilled water and dissolved in 100 mM CAPS and 0.05% β-mercaptoethanol, pH 10.6, for 2 h at 37 °C, and insoluble material was removed by centrifugation 10000*g* for 10 min. Cry11Ba protoxin was activated to toxin by incubation with bovine pancreatic trypsin (Sigma) at a mass ratio of 50:1 (toxin:trypsin) for 2 h at 37 °C. Activated Cry11Ba was purified by fast protein liquid chromatography, using a Bio-Scale mini High Q cartridge (Bio-Rad, Richmond, CA).

Cloning and Expression of APN Fragments. Two pairs of specific primers listed in Table 1 were designed according to the sequence of AgAPN2 (GenBank accession number EU827528). Polyermase chain reaction (PCR) amplifications were performed using pGEM-AgAPN2 (*21*) as template with 30 cycles of 94 °C for 30 s, 58 °C for 30 s, and 72 °C for 1 min. The resulting PCR fragments were cloned into the protein expression vector pET-30a (+) (Novagen, Madison, WI) through *Nde*I/*Xho*I cuts to yield plasmids pET-AgAPN2ta and pET-AgAPN2tb. The coding sequences were confirmed by sequencing. The pET- constructs were transformed into *E. coli* strain BL21-CodonPlus (DE3)/pRIL (Stratagene, La Jolla, CA). The APN peptides were overexpressed in *E. coli* as inclusion bodies which were stored at 5 °C in deionized water until needed. The protein components of inclusion bodies were examined by 12% SDS−PAGE and Coomassie blue G-250 staining. For the following binding assays, inclusion bodies were centrifuged and solubilized in 8 M urea and 20 mM Na_2CO_3, pH 9.6. Soluble AgAPN peptides were purified by a HiTrap Ni^{2+}-chelating HP column (GE Healthcare, Piscataway, NJ) according to the manufacturer's manual and dialyzed against 10 mM Na_2CO_3, pH 9.6.

Circular Dichroism (CD) Spectroscopy. Inclusion bodies of AgAPN2ta and AgAPN2tb were solubilized in 8 M urea, 20 mM Na_2HPO_4, and 0.5 M NaCl, pH 7.6, and dialyzed against 6, 4, 2, 1, 0.5, 0.1, and 0 M urea in 10 mM carbonate buffer, pH 9.6. Proteins were purified by a HiTrap Ni^{2+}-chelating HP column (GE Healthcare, Piscataway, NJ) according to the manufacturer's manual. Purified AgAPN2ta and AgAPN2tb peptides were dialyzed in 10 mM Na_2CO_3, pH 9.6, at a concentration of 10 μM to remove imidazole. CD spectroscopy measurements were performed according to ref *22*. The acquired CD spectra were analyzed by CDSSTR algorithms (*25*−*27*) using the DICHROWEB server (http://dichroweb.cryst.bbk.ac.uk/html/home.shtml). Secondary structure assignments were made as described previously (*28*).

In-Frame Deletion of AgAPN2ta and AgAPN2tb. Specific primers for cloning AgAPN2ta/Del1 and AgAPN2tb/Del1 were designed (Table 1). PCR amplifications and transformations were performed as described in ref *21*. The strategy for constructing other in-frame deletions was based on the Stratagene QuickChange method described previously (*22*, *29*). Briefly, 5′- and 3′-primer pairs were designed that were complementary to the region to be deleted and have an endonuclease cleavage site at each end (Table 1). PCR was performed using Elongase enzyme mix (Invitrogen, Carlsbad, CA) with pET-AgAPN2ta or pET-AgAPN2tb plasmid as template. The PCR product was gel-purified, digested with *Dpn*I and the corresponding endonuclease, and then transformed into *E. coli* BL21 after ligation. The coding regions of all mutated plasmids were sequenced. Culture growth, protein induction, and purification of expressed peptides are described in ref *21*. The expressed AgAPN2 peptides have a stretch of contiguous amino acid residues deleted that were replaced with E and F or K and L due to the introduction of the *Eco*RI or *Hin*dIII site in the DNA sequence.

Mosquito Bioassays. The colony of *A. gambiae* (CDC G3 strain) was maintained as described previously (*21*). Soluble Cry11Ba was mixed with APN inclusion bodies at 1:100 toxin: peptide molar ratio. Cry11Ba alone or toxin−peptide mixtures were transferred to wells of a six-well Costar culture plate (Corning). Ten early fourth instar larvae were added to each well and the plates incubated at 27 °C. Each treatment was in triplicate, and the bioassays were conducted at least three times, and there was a control of inclusion bodies alone. Larval mortality was recorded after 24 h.

Microtiter Binding Assays. The biotinylation and dialysis of APN peptides were described previously (*21*). Microtiter plates (high-binding 96-well, Immulon 2HB; Thermo Fisher Scientific Inc., Waltham, MA) were coated overnight at 4 °C with 1.0 μg of Cry11Ba/well in 100 μL of coating buffer (100 mM Na_2CO_3, pH 9.6) and blocked as described in ref *21*. In a saturation binding assay, biotinylated AgAPN2 peptides were diluted to the desired concentrations (0.5−100 nM) in 100 μL of coating buffer (100 mM Na_2CO_3, pH 9.6) with or without a 1000-fold molar excess of nonlabeled AgAPN2 peptides. In a competition binding assay, 20 nM biotinylated AgAPN2 peptides were mixed with increasing concentrations of unlabeled AgAPN2 peptides. Other reaction conditions were according to Zhang et al. (*21*).

Brush Border Membrane Vesicle (BBMV) Preparation and Binding Assays. Frozen *A. gambiae* fourth instar larvae were kindly provided by the Malaria Research and Reference Reagent Resource Center (MR4) and stored in −80 °C until use. BBMVs were prepared from the whole body of fourth instar larvae by $MgCl_2$ precipitation according to Silva-Filha et al. (*30*) and stored in aliquots at −80 °C. Protein was measured by Bio-Rad protein assay using bovine serum albumin (BSA) as standard (*31*). APN activity (*32*), a marker for brush border membranes, was enriched about 5-fold for the final BBMV preparation compared to the initial crude larval homogenate.

Trypsinated Cry11Ba (10 μg) was labeled with 0.5 mCi of $Na^{125}I$ (PerkinElmer) using the chloramine-T method (*33*), and specific activity was 19.1 μCi/μg of input toxin. BBMV binding assays were performed according to Garczynski et al. (*33*). For homologous and heterologous competition assays, duplicate samples of ^{125}I-Cry11Ba toxin in increasing amounts were mixed with 10 μM unlabeled APN peptides and incubated in binding buffer (20 mM Na_2CO_3, pH 9.6) at room temperature for 2 h. Samples were then added with 8 μg of BBMVs that were preblocked for 2 h at room temperature in 25 μL of blocking buffer (20 mM Na_2CO_3, pH 9.6, 0.15 M NaCl, 0.1% Tween-20, 1.5% BSA) and then incubated at 4 °C for 18 h. Binding reactions were stopped by centrifugation and pellets washed twice with 1 mL of ice-cold binding buffer. Radioactivity of the final pellets was measured with a Beckman model Gamma 4000 detector. Each binding assay was repeated twice.

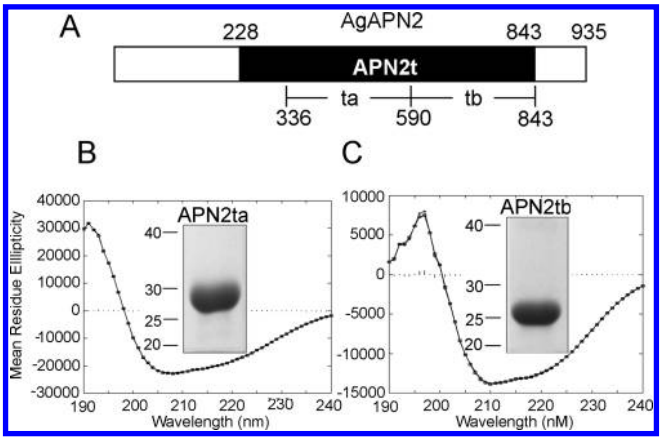

FIGURE 1: Purified AgAPN2ta and -2tb fragments demonstrate partially folded structures. (A) Schematic representation of the truncations of AgAPN2. (B) Far-UV CD spectrum (190−240 nm) of AgAPN2ta peptide. (C) Far-UV CD spectrum (190−240 nm) of AgAPN2tb peptide. Mean residue ellipticity was measured in deg cm^2 dmol^{-1} residue^{-1}. (Insets) SDS−PAGE of purified AgAPN2ta and -2tb.

Statistical Analysis. Sigma Plot software version 11.0 (SPSS Science, Chicago, IL) was used for statistical analysis of all data. Results are presented as the mean ± SEM. One-way ANOVA was used to evaluate statistical significance. An asterisk symbol above the error bars indicates significant difference between means ($P < 0.001$).

RESULTS

AgAPN2ta and AgAPN2tb Peptides Are Structurally Refolded in Solution. Aminopeptidase AgAPN2 was recently identified as a candidate receptor of Cry11Ba in *A. gambiae* larval midgut (*21*). A 70-kDa peptide fragment of AgAPN2t (^{228}G−V^{843}) binds Cry11Ba with a high affinity (K_d = 6.4 nM) and inhibits toxicity to larvae. The goals of this study were to locate Cry11Ba binding region(s) on AgAPN2t and test for a correlation between toxin binding and toxicity inhibition. We divided AgAPN2t into segments AgAPN2ta and AgAPN2tb and expressed the peptides in *E. coli* for isolation and use in assays (Figure 1A). Panels B and C (inset) of Figure 1 show lanes from a SDS gel of 30-kDa AgAPN2ta and 28-kDa AgAPN2tb peptides after solubilization from inclusion bodies and purification by immobilized nickel chromatography. The peptides were dialyzed into 10 mM Na_2CO_3, pH 9.6, conditions approximating the alkaline environment of mosquito midgut, and analyzed for peptide secondary structures by far-UV CD spectroscopy (Figure 1B,C). The CD spectra indicated the composition of AgAPN2ta was 52% α-helix (33% ordered, 19% disordered), 16% β-strand (8% ordered, 8% disordered), 13% turns, and 17% unordered, while AgAPN2tb was 42% α-helices (24% ordered, 18% disordered), 21% β-strand (13% ordered, 8% disordered), 17% turns, and 20% unordered. Therefore, AgAPN2ta and AgAPN2tb fragments clearly retain some secondary structure in the alkaline buffer. Peptide fragments did not have aminopeptidase activity (data not shown).

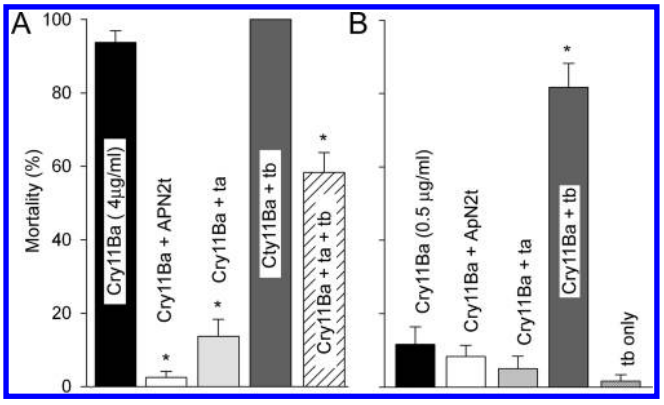

FIGURE 2: AgAPN2ta inhibits and AgAPN2tb enhances Cry11Ba toxicity to *A. gambiae* larvae. Soluble Cry11Ba alone or with APN inclusions at a toxin/peptide molar ratio of 1:100 were diluted in plastic plates containing 2 mL of deionized water and tested against ten early fourth instar larvae of *A. gambiae*. Each treatment was in triplicate, and the bioassays were conducted three times. Larval mortality was recorded after 24 h. (A) Mean percent mortality (±SE) of larval mosquitoes treated with 4 μg/mL Cry11Ba when APN inclusion bodies were absent or present. (B) Mean percent mortality (±SE) of larval mosquitoes treated with 0.5 μg/mL Cry11Ba when APN inclusion bodies were absent or present. An asterisk indicates a significant difference between larval mortality with Cry11Ba treatment alone and that with Cry11Ba plus peptide treatment at the same toxin dose (one-way ANOVA, $P < 0.001$).

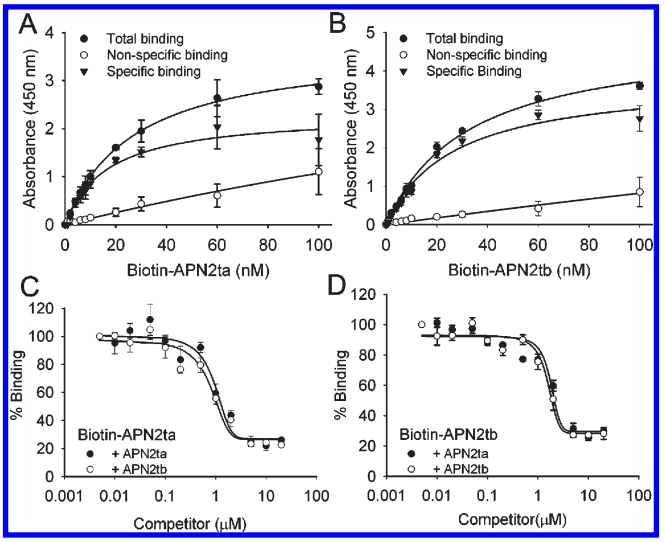

FIGURE 3: Analyses of the interaction between Cry11Ba and truncated APN peptides. The binding affinities (K_d) of AgAPN2ta (A) or AgAPN2tb (B) to Cry11Ba were determined by saturation binding assays using increasing nanomolar concentrations of biotinylated peptides with a 1000-fold molar excess of unlabeled homologous peptides. (C, D) Shared bindings of AgAPN2ta and AgAPN2tb to Cry11Ba were determined by competitive binding assays using 20 nM biotinylated AgAPN2ta or -2tb peptides as probes with increasing concentrations of nonlabeled homologous or heterologous peptides.

AgAPN2ta Inhibits and AgAPN2tb Enhances Cry11Ba Toxicity to A. gambiae Larvae, and Both Peptides Bind Trypsinized Cry11Ba. The effects of AgAPN2ta and AgAPN2tb peptides on Cry11Ba toxicity were tested by feeding fourth instar larvae of *A. gambiae* Cry11Ba toxin alone or in combination with AgAPN2t, -2ta, or -2tb inclusion bodies. As expected from our previous study, AgAPN2t peptide blocked 98% of the Cry11Ba potency at 4 μg of Cry11Ba/mL (*21*) (Figure 2A). While -2ta reduced larval mortality by 85%, -2tb showed no significant effect in larval mortality (Figure 2A). A 1:1 mixture of -2ta and -2tb inclusions produced an intermediate level of toxicity inhibition (Figure 2A). As shown in Figure 2B, an enhancement effect of AgAPN2tb inclusions was significant at a low Cry11Ba concentration (0.5 μg/mL) where the addition of -2tb inclusions increased larval mortality from 11.7 ± 4.8% to 81.7 ± 6.5% ($P < 0.001$). These peptide AgAPN2tb inclusion bodies alone were not toxic to *A. gambiae* larvae (Figure 2B).

Since 70-kDa AgAPN2t binds Cry11Ba with high affinity as measured in an ELISA microplate binding assay, we tested binding of AgAPN2ta and -2tb peptides in the same saturation binding format (*21*). Plates were coated with trypsinized Cry11Ba and probed with biotin−AgAPN2ta or biotin−AgAPN2tb peptide alone or with excess unlabeled homologous peptide (Figure 3A,B). Using a one-site saturation fit model, the calculated K_d for AgAPN2ta and AgAPN2tb binding to Cry11Ba was 16.7 ± 4.8 nM and 26.4 ± 3.6 nM, respectively. Although both truncated AgAPN2t peptides bound toxin, the affinities were lower than the affinity (K_d = 6.4 ± 1.4 nM) previously determined for the 70-kDa AgAPN2t binding to Cry11Ba (*21*).

Reasoning that AgAPN2ta and -2tb peptides may bind distinct sites on Cry11Ba, we biotinylated AgAPN2ta and AgAPN-2tb and measured binding to immobilized Cry11Ba alone and in the presence of increasing concentrations (5 nM−20 μM) of unlabeled homologous or heterologous peptides. As shown in Figure 3C,D the competition curves are similar for biotin−AgAPN2ta and biotin−AgAPN2tb probes and for homologous and heterologous competitors, a result indicative of a shared binding site or sites on Cry11Ba.

Toxicity Inhibition Depends on Cry11Ba Binding to the N-Terminal Region of AgAPN2ta. The correlation between AgAPN2ta inhibition of Cry11Ba toxicity and toxin binding was tested by producing in-frame truncations that deleted 10-kDa segments of AgAPN2ta resulting in the 20-kDa peptides AgAPN2ta/Del1, -2ta/Del2, and -2ta/Del3 (Figure 4A). Figure 4B shows a stained SDS gel of peptides after partial purification from *E. coli* inclusion bodies. Cry11Ba was fed alone to larvae or with a 1:100 ratio of AgAPN2ta or deleted peptide inclusion bodies, and mortality was scored after 24 h. Peptide AgAPN2ta inclusion bodies reduced larval mortality from 93.8 ± 3.2% to 13.8 ± 4.6% ($P < 0.001$), and peptides -2ta/Del2 and -2ta/Del3 reduced mortality to 8.8 ± 4.0% and 5.0 ± 2.7%, respectively. The addition of AgAPN2ta/Del1 inclusion bodies did not alter Cry11Ba toxicity, indicating that the N-terminal 10-kDa AgAPN2ta ($^{336}S-P^{420}$) is critical to AgAPN2ta inhibition of Cry11Ba toxicity (Figure 4C). Considering that structural composition may affect peptide functional properties, the CD spectra of -2ta/Del1 peptide which had lost toxicity inhibition and the inhibitory peptide -2ta/Del2 were measured (Figure 4D,E). The spectral data for -2ta/Del1 indicated a composition of 63% α-helix (46% ordered,17% disordered), 14% β-strand (6% ordered, 8% disordered), 12% turns, and 11% unordered and spectra of -2ta/Del2 a composition of 54% α-helix (33% ordered, 21% disordered), 12% β-strand (7% ordered, 5% disordered), 13% turns, and 21% unordered. There was a 10% increase in α-helical composition in -2ta/Del1 relative to the inhibitory -2ta/Del2 and -2ta peptides.

Since biotin−AgAPN2ta binds Cry11Ba in a specific and competitive manner, we tested the abilities of each deleted AgAPN2ta peptide to compete for binding to Cry11Ba in an ELISA. While 20 nM input biotin−AgAPN2ta was displaced by increased concentrations (5 nM−20 μM) of unlabeled AgAPN2ta, -2ta/Del2, and -2ta/Del3 (Figure 5A), AgAPN2ta/Del1 was less effective at reducing bound biotin−AgAPN2ta. The result

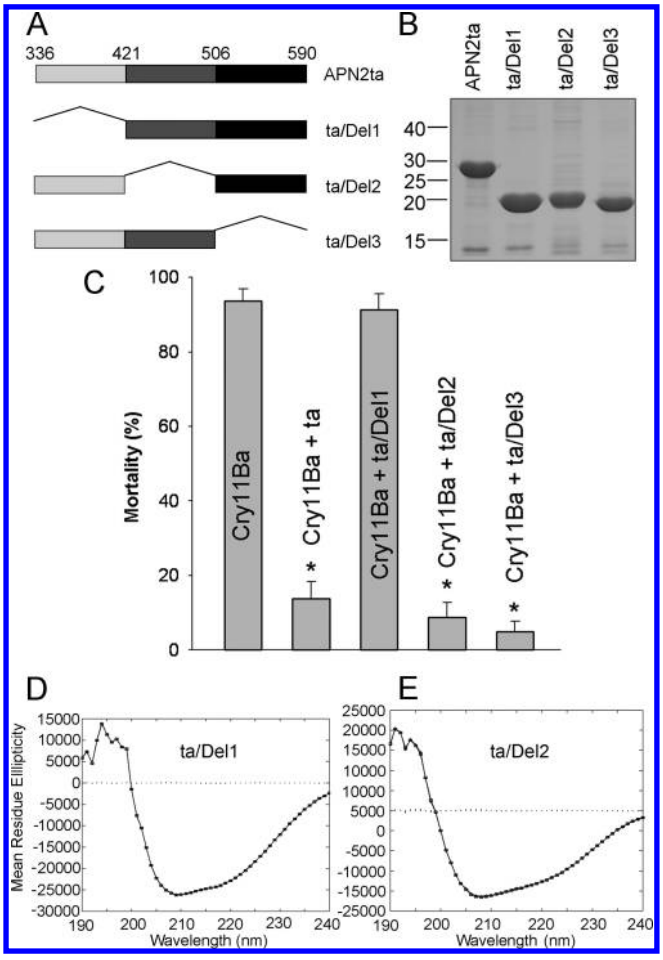

FIGURE 4: A 10-kDa segment deletion in the N-terminus causes AgAPN2ta loss of inhibitory effect to Cry11Ba toxicity. (A) Schematic representation of the construction of in-frame deletions of AgAPN2ta. (B) Partially purified recombinant AgAPN2ta and its deletions were resolved by SDS−PAGE and stained with Coomassie blue. (C) Mean percent mortality (±SE) of larval mosquitoes treated with 4 μg/mL Cry11Ba when APN inclusion bodies were absent or present. An asterisk indicates a significant difference between larval mortality with Cry11Ba treatment alone and that with Cry11Ba plus peptide treatment at the same toxin dose (one-way ANOVA, $P < 0.001$). (D, E) Far-UV CD spectrum (190−240 nm) of AgAPN2ta/Del peptides.

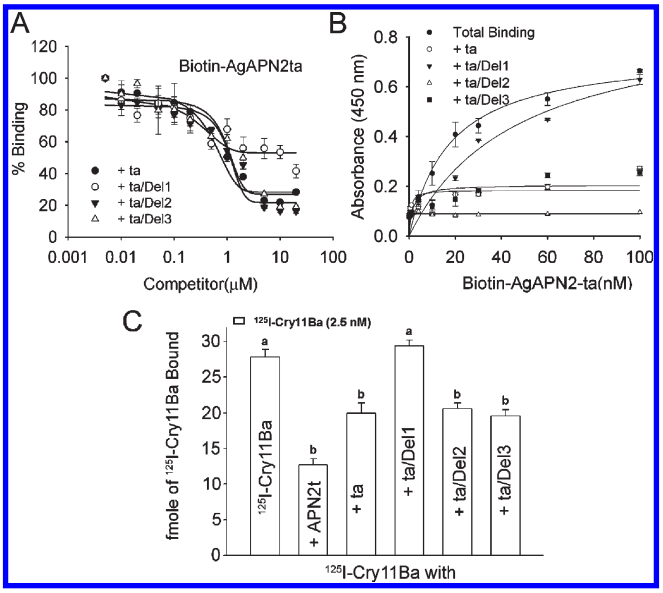

FIGURE 5: Analysis of the interaction of AgAPN2ta and its deletions to Cry11Ba. (A) AgAPN2ta/Del1 partially compete the binding of AgAPN2ta to Cry11Ba in competition binding assays. Microtiter plates coated with 1 μg of trypsinized Cry11Ba were incubated with 20 nM biotinylated AgAPN2ta protein and increasing concentrations of unlabeled AgAPN2ta or AgAPN2ta derivatives. (B) AgAPN2ta derivatives compete the binding of AgAPN2ta to Cry11Ba in saturation binding assays. Microplates coated with 1 μg of trypsinized Cry11Ba were incubated with increasing nanomolar concentrations of biotinylated AgAPN2ta peptide alone or with a 1000-fold molar excess of unlabeled peptides. (C) Average (±SE) binding of 2.5 nM ^{125}I-Cry11Ba to 8 μg of *A. gambiae* BBMV in the presence or absence of 10 μM competitors. Different letters above the error bars indicate significant differences between means.

that AgAPN2ta/Del1 reduced biotin−AgAPN2ta binding to about half that of the other AgAPN2ta peptides suggested the removal of a binding site from AgAPN2ta by the Del1 deletion and that a second binding site(s) is contained in regions 2 and 3 of AgAPN2ta. Further evidence of loss of a Cry11Ba binding site in AgAPN2ta/Del1 is shown in Figure 5B, where AgAPN2ta/Del1 at a 1000-fold ratio to biotin−AgAPN2ta minimally reduced binding to Cry11Ba in a saturation assay.

Since AgAPN2t reduced ^{125}I-Cry11Ba binding to BBMV prepared from *A. gambiae* larvae (*21*), we tested AgAPN2ta and its deleted versions as competitors of ^{125}I-Cry11Ba binding to BBMV (Figure 5C). As expected (*21*), unlabeled 70-kDa AgAPN2t fragment competed 54.6% of the ^{125}I-Cry11Ba binding, reducing the toxin bound from 27.86 ± 1.03 to 12.65 ± 0.92 fmol. The 30-kDa AgAPN2ta peptide and the deleted peptides -2ta/Del2 and -2ta/Del3 reduced bound Cry11Ba to 19.95 ± 1.44 fmol, 20.59 ± 0.76 fmol for -2ta/Del2, and 19.51 ± 0.90 fmol, respectively. In contrast, the addition of AgAPN2ta/Del1, the peptide with the deleted Cry11Ba binding site, did not change ^{125}I-Cry11Ba binding to *A. gambiae* BBMV.

AgAPN2ta/Del1 peptide with residues ^{336}S−P^{420}of AgAPN2 deleted had lost a Cry11Ba binding site and the ability to compete with Cry11Ba binding to BBMV and reduce Cry11Ba toxicity to *A. gambiae* larvae. These results are evidence that residues ^{336}S−P^{420} contain an epitope that is critical for Cry11Ba binding to aminopeptidase AgAPN2.

Toxicity Enhancement Is Correlated with a Central 10-kDa Region of AgAPN2tb and Increased ^{125}I-Cry11Ba Binding to BBMV. As shown in Figures 2 and 3, AgAPN2tb bound Cry11Ba with high affinity and enhanced Cry11Ba toxicity. In-frame deleted peptides of AgAPN2tb were constructed to identify a region of AgAPN2tb critical to enhancement of Cry11Ba toxicity. Peptides AgAPN2tb/Del1, -2tb/Del2, and -2tb/Del3 had fragments deleted from the N-terminal (^{591}G−I^{661}), middle (^{676}I−W^{760}), or C-terminal (^{761}N−V^{843}) region, respectively, of AgAPN2tb (Figure 6A,B). Cry11Ba alone at 0.5 μg/mL killed 10.0 ± 2.6% of the *A. gambiae* larvae. When the same amount of toxin was mixed with a 100-fold excess of AgAPN2tb, larval mortality attained 82.7 ± 6.5%. The addition of 100-fold -2tb/Del1 or -2tb/Del3 also caused a significant toxicity enhancement ($P < 0.001$) to 61.7 ± 4.9% and 76.7 ± 6.7% mortality, respectively. In contrast, AgAPN2tb/Del2 peptide added to Cry11Ba resulted in 18.0 ± 4.9% mortality, a level not statistically different from Cry11Ba alone (Figure 6C). These results demonstrated that the middle region of AgAPN2tb (^{676}I−W^{760}) was essential for the enhancing effect mediated by AgAPN2tb peptide. The structure of the toxicity enhancing -2tb/Del1 fragment deduced from CD spectra (Figure 6D) was 55% α-helix (36% ordered, 19% disordered), 20% β-strand (11% ordered, 9% disordered), 10% turns, and 15% unordered, while the

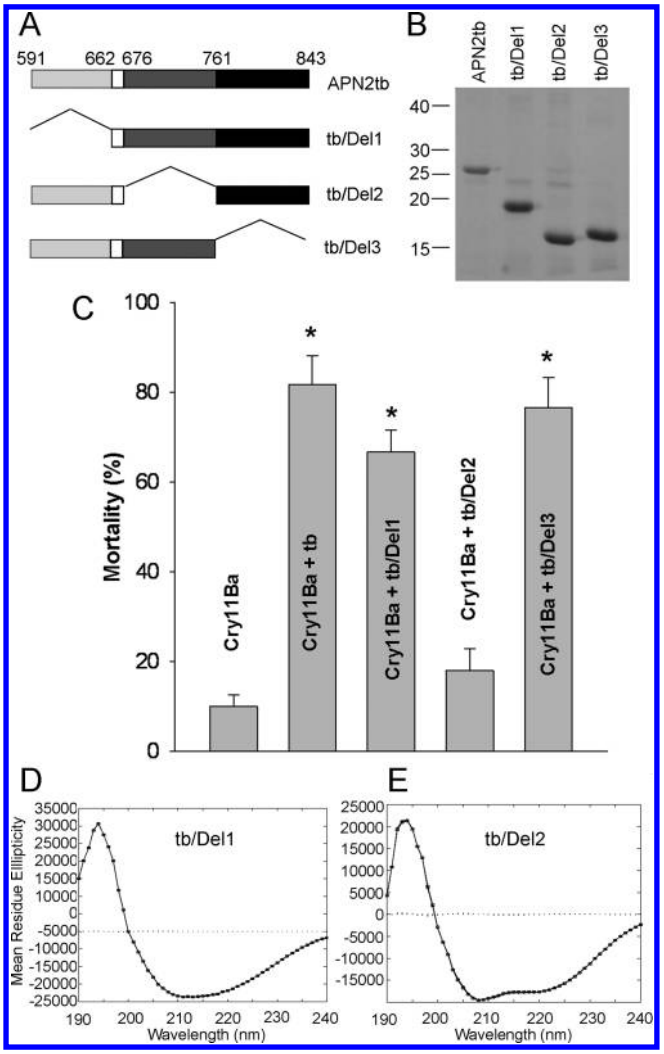

FIGURE 6: A deletion of 85 amino acids in the central region causes AgAPN2tb loss of enhancement effect to Cry11Ba toxicity. (A) Schematic representation of the construction of in-frame deletions of AgAPN2tb. (B) Partially purified recombinant AgAPN2tb and its deletions were resolved by SDS−PAGE and stained with Coomassie blue. (C) Mean percent mortality (±SE) of larval mosquitoes treated with 0.5 μg/mL Cry11Ba when APN inclusion bodies were absent or present. An asterisk indicates a significant difference between larval mortality with Cry11Ba treatment alone and that with Cry11Ba plus peptide treatment at the same toxin dose (one-way ANOVA, $P < 0.001$). (D, E) Far-UV CD spectrum (190−240 nm) of AgAPN2tb/Del peptides.

composition of -2b/Del2 calculated from CD spectra (Figure 6E) was 63% α-helix (38% ordered, 25% disordered), 9% β-strand (4% ordered, 5% disordered), 15% turns, and 14% unordered. The two -2tb/Del peptides had slightly more α-helical composition than the parental -2tb peptide.

To locate the toxin binding region in AgAPN2tb, we coated microtiter plate wells with Cry11Ba and probed with biotin−AgAPN2tb alone or with various concentrations (5 nM−20 μM) of unlabeled AgAPN2tb or its deletions. Figure 7A shows the results of the competition binding experiment where -2tb/Del2 displaced biotinylated AgAPN2tb binding to a level similar to that of unlabeled AgAPN2tb, whereas -2tb/Del1 and -2tb/Del3 only partially competed binding of AgAPN2tb. A deletion in the middle region of AgAPN2tb did not alter the binding to Cry11Ba while deletions in either end resulted in the partial loss of toxin binding, suggesting that Cry11Ba binding sites are localized on both N-terminal and C-terminal regions of AgAPN2tb.

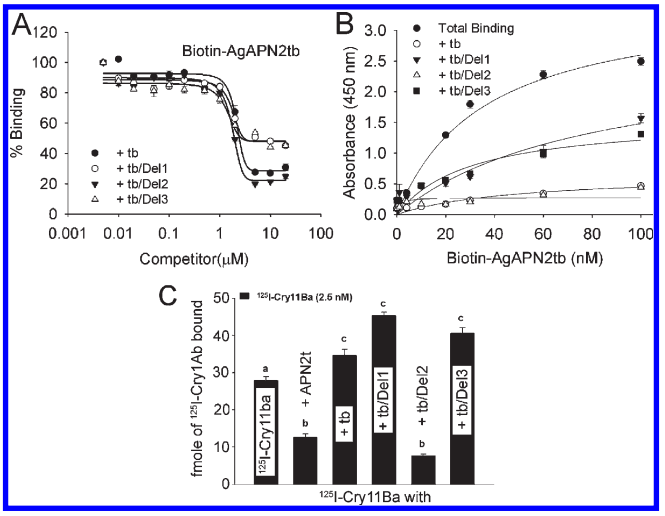

FIGURE 7: AgAPN2tb/Del2 loses the ability to enhance Cry11Ba toxicity while still binds to Cry11Ba. (A) AgAPN2tb derivatives compete AgAPN2tb binding to Cry11Ba in competition binding assays. Microtiter plates coated with 1 μg of trypsinized Cry11Ba were incubated with 20 nM biotinylated AgAPN2ta protein and increasing concentrations of unlabeled AgAPN2tb or AgAPN2tb derivatives. (B) AgAPN2tb derivatives compete the binding of AgAPN2tb to Cry11Ba in saturation binding assays. Microplates coated with 1 μg of trypsinized Cry11Ba were incubated with increasing nanomolar concentrations of biotinylated AgAPN2tb peptide alone or with a 1000-fold molar excess of unlabeled peptides. (C) Average (±SE) binding of 2.5 nM ^{125}I-Cry11Ba to 8 μg of *A. gambiae* BBMV in the presence or absence of 10 μM competitors. Different letters above the error bars indicate significant differences between means.

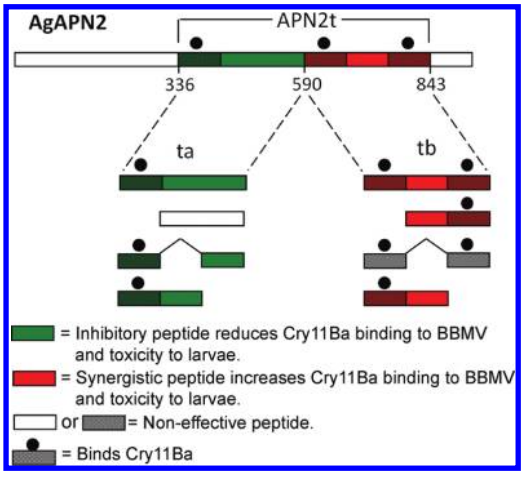

FIGURE 8: Schematic diagram of various AgAPN2 deleted regions and their effects on Cry11Ba binding and toxicity to larval mosquitoes.

AgAPN2tb/Del2 had lost the ability to enhance Cry11Ba toxicity yet bound Cry11Ba to the same extent as AgAPN2tb. We hypothesized that AgAPN2tb might affect Cry11Ba binding to BBMV. Therefore, we measured ^{125}I-Cry11Ba binding to BBMV in the presence of AgAPN2tb or its deleted derivatives. As shown in Figure 7C, AgAPN2tb, -2tb/Del1, and -2tb/Del3 increased Cry11Ba binding to BBMV by 24%, 62%, and 45%, respectively. In contrast, binding of ^{125}I-Cry11Ba to BBMV was decreased 50% with 70-kDa AgAPN2t and 72% with 18-kDa AgAPN2tb/Del2.

In summary and as shown schematically in Figure 8, bioassay experiments with AgAPN2tb, -2tb/Del1, and -2tb/Del3 showed enhanced Cry11Ba toxicity to larvae, and the same peptides bound Cry11Ba and increased ^{125}I-Cry11Ba binding to BBMV.

In contrast, the deleted peptide AgAPN2tb/Del2 bound Cry11Ba but reduced Cry11Ba binding to BBMV and had no effect on toxicity. Although the central region of AgAPN2tb is not involved in peptide binding to Cry11Ba, the region is necessary for increased Cry11Ba binding to BBMV and increased Cry11Ba toxicity to larvae.

DISCUSSION

In this work, we identified two fragments of the Cry11Ba binding protein AgAPN2 that bind toxin yet have opposite effects on Cry11Ba binding to BBMV and toxicity to larvae (Figure 8). The 30-kDa AgAPN2ta peptide retains the inhibitory effect of 70-kDa AgAPN2t peptide. AgAPN2ta binds Cry11Ba with high affinity (K_d = 16.7 nM), an affinity comparable to the binding of the parental AgAPN2t peptide (K_d = 6.4 nM). Using a scanning-block deletion method, we localized the Cry11Ba binding site between ^{336}Ser and ^{420}Pro. The AgAPN2ta/Del1 peptide without this region loses the ability to inhibit Cry11Ba binding to BBMV and neutralize toxicity to larvae (Figures 4 and 5). Our data support the conclusion that the ^{336}Ser to ^{420}Pro region of AgAPN2 contains a binding epitope that is involved in Cry11Ba interaction with AgAPN2 and possibly other Cry11Ba binding molecules on the larval brush border. This 85 amino acid region shows no sequence similarity to the reported Cry1A binding site on *B. mori* APN and the Cry11Aa binding area on *A. aegypti* APN (*19*, *20*), suggesting that the amino acid primary structure in this region may play an important role in recognition by Cry11Ba toxin and may be a determinant of Cry11Ba larval specificity.

We unexpectedly discovered that the C-terminal region of AgAPN2t synergized Cry11Ba toxicity in bioassays with mixtures of Cry11Ba and AgAPN2tb inclusions. A similar *in vivo* approach led to the discovery of the CR12-MPED fragment from *M. sexta* cadherin Bt-R1 as a synergist of Cry1A toxicity to lepidopteran larvae (*22*). In the case of the CR12-MPED peptide, the synergism requires the Cry1Ab-binding epitope. Removal of the eight amino acid binding epitope on CR12-MPED resulted in loss of binding to Cry1A and its synergistic ability. In our experiments, we showed that AgAPN2tb bound Cry11Ba with nanomolar affinity (K_d = 26.4 nM) (Figure 3B), a value comparable to the high-affinity binding of Cry1Ab to cadherin peptide CR12-MPED (K_d = 9.17 nM). Thus, we hypothesized that the lack of insecticidal synergy by AgAPN2tb/Del2 peptide would correlate with loss of a Cry11Ba binding site. However, AgAPN2tb/Del2 proved to be an effective competitor of AgAPN2tb binding to Cry11Ba in both competition and saturation ELISA binding assays (Figures 6 and 7). In contrast, the AgAPN2tb/Del1 and -2tb/Del3 synergistic peptides each had a deleted Cry11Ba binding site which resulted in the ability to compete only 50% of the biotin−AgAPN2tb bound to Cry11Ba (Figure 7A,B). Rather than affecting peptide binding to Cry11Ba, deletion of the middle region of AgAPN2tb, as in AgAPN2tb/Del2 peptide, resulted in loss of enhanced ^{125}I-Cry11Ba binding to BBMV. Synergism of Cry11Ba binding and toxicity by a derivative of AgAPN2tb appears to require the middle Del2 region and either the N- or C-terminal regions of AgAPN2tb. One explanation of the observed synergism is that the fragment deleted in AgAPN2tb/Del2 could act as a "bridge" to vector toxins to receptors on the midgut brush border. The concept of bridge was proposed to account for CR12-MPED synergizing Cry1Ab toxicity, whereby CR12-MPED binding to BBMV increases the probability of toxin interaction with Cry1A receptors (*22*). However, it is important to note that CR12-MPED binds *M. sexta* BBMV with high affinity (32 nM), whereas AgAPN2tb and its derivatives only bind *A. gambiae* BBMV in an unsaturable manner (Supporting Information Figure S1). The inhibitory AgAPN2ta bound BBMV, but to a lesser extent than -2tb peptide (Supporting Information Figure S1). An argument against a "bridge" model is that AgAPN2tb/Del2, which has lost the enhancing effect, bound BBMV (Supporting Information Figure S1). An alternative explanation for toxicity enhancement is that AgAPN2tb could modify interactions between Cry11Ba and receptor molecules on epithelial cells of mosquito midgut. Studies with *M. sexta* synergist CR12-MPED have shown that it is able to promote toxin oligomerization, an essential step for Cry1A activity in the pore-formation model (*34*, *35*). A cadherin fragment from *Helicoverpa armigera* was also reported to facilitate oligomer formation and enhance Cry1Ac toxicity (*36*). However, no significant Cry11Ba oligomerization was observed with the addition of AgAPN2tb in the presence of trypsin and BBMV (Supporting Information Figure S2). Recently, an updated pore-formation model proposed that, depending on the oligomeric state of the toxin, Cry1A binds cadherin and APN in a sequential "ping-pong" fashion (*37*). Therefore, different interactions of toxin with two proteins may implicate different mechanisms of synergism for APN and cadherin proteins. In addition, BBMV binding assays in this study identified that the peptides capable of enhancing Cry11Ba toxicity could also increase Cry11Ba binding to BBMV (Figure 7C). On the contrary, a cadherin fragment was found to synergize mosquitocidal Cry4Ba toxicity but inhibits toxin binding to BBMV (*24*). If these initial observations are further validated, it may add additional complexity to the synergistic mechanisms in mosquitoes.

In this research, we have empirically determined that two fragments of AgAPN2 bound Cry11Ba with high affinity. Competitive binding assays using two APN fragments as homologous or heterologous competitors indicated that the two APN fragments share the same binding site(s) on Cry11Ba. It is possible that Cry11Ba binds multiple sites on AgAPN2. *Manduca* APN and *Heliothis* APN are reported to bind Cry1A with 2:1 toxin:receptor stoichiometries (*14*, *17*). Although speculative, it is possible that Cry11Ba binds sequentially to two sites on AgAPN2 in a 1:1 toxin:receptor ratio, as described for the interaction between Cry1Ac and *L. dispar* APN, whereby Cry1Ac binding to site 1 initiates a fast reversible interaction with the receptor that is followed by a high-affinity binding to site 2 (*38*). The authors proposed that Cry toxin undergoes a conformational change upon binding to APN site 2 that leads to an irreversible insertion into the target membrane. It remains to be determined how toxin binding to receptor triggers the event. Our work has localized the Cry11Ba binding regions on AgAPN2. We have also identified a nontoxin binding region on AgAPN2 that is crucial for the enhancement of Cry11Ba toxicity. Further investigation of the interaction between Cry11Ba and these two regions on AgAPN2 will help to better understand the mechanism of toxin pore formation on the cell membrane.

ACKNOWLEDGMENT

We thank Ramona Bieber Urbauer for assistance in CD spectroscopy and Sue MacIntosh and Drs. Mohd Amir Abdullah, Mark Brown, and Judith Willis for reviewing versions of the manuscript.

SUPPORTING INFORMATION AVAILABLE

AgAPN2ta, AgAPN2tb, and AgAPN2tb/Del2 bind to BBMV in a nonsaturable and nonspecific manner; AgAPN2ta and AgAPN2tb do not significantly promote Cry11Ba oligomerization. This material is available free of charge via the Internet at http://pubs.acs.org.

REFERENCES

1. Lacey, L. A. (2007) *Bacillus thuringiensis* serovariety *israelensis* and *Bacillus sphaericus* for mosquito control. *J. Am. Mosq. Control Assoc. 23*, 133–163.
2. Porter, A. G., Davidson, E. W., and Liu, J. W. (1993) Mosquitocidal toxins of bacilli and their genetic manipulation for effective biological control of mosquitoes. *Microbiol. Rev. 57*, 838–861.
3. Delécluse, A., Rosso, M. L., and Ragni, A. (1995) Cloning and expression of a novel toxin gene from *Bacillus thuringiensis* subsp. *jegathesan* encoding a highly mosquitocidal protein. *Appl. Environ. Microbiol. 61*, 4230–4235.
4. Li, J., Carroll, J., and Ellar, D. J. (1991) Crystal structure of insecticidal δ-endotoxin from *Bacillus thuringiensis* at 2.5 Å resolution. *Nature 353*, 815–821.
5. Boonserm, P., Davis, P., Ellar, D. J., and Li, J. (2005) Crystal structure of the mosquito-larvicidal toxin Cry4Ba and its biological implications. *J. Mol. Biol. 348*, 363–382.
6. Boonserm, P., Mo, M., Angsuthanasombat, C., and Lescar, J. (2006) Structure of the functional form of the mosquito larvicidal Cry4Aa toxin from *Bacillus thuringiensis* at a 2.8-angstrom resolution. *J. Bacteriol. 188*, 3391–3401.
7. Galitsky, N., Cody, V., Wojtczak, A., Ghosh, D., Luft, J. R., Pangborn, W., and English, L. (2001) Structure of the insecticidal bacterial delta-endotoxin Cry3Bb1 of *Bacillus thuringiensis*. *Acta Crystallogr., Sect. D: Biol. Crystallogr. 57*, 1101–1109.
8. Grochulski, P., Masson, L., Borisova, S., Pusztai-Carey, M., Schwartz, J.-L., Brousseau, R., and Cygler, M. (1995) *Bacillus thuringiensis* CryIA(a) insecticidal toxin: crystal structure and channel formation. *J. Mol. Biol. 254*, 447–464.
9. Morse, R. J., Yamamoto, T., and Stroud, R. M. (2001) Structure of Cry2Aa suggests an unexpected receptor binding epitope. *Structure* (*Cambridge*) *9*, 409–417.
10. Pigott, C. R., and Ellar, D. J. (2007) Role of receptors in *Bacillus thuringiensis* crystal toxin activity. *Microbiol. Mol. Biol. Rev. 71*, 255–281.
11. Bravo, A., Gómez, I., Conde, J., Muñoz-Garay, C., Sánchez, J., Miranda, R., Zhuang, M., Gill, S. S., and Soberón, M. (2004) Oligomerization triggers binding of a *Bacillus thuringiensis* Cry1Ab pore-forming toxin to aminopeptidase N receptor leading to insertion into membrane microdomains. *Biochim. Biophys. Acta 1667*, 38–46.
12. Zhang, X., Candas, M., Griko, N. B., Taussig, R., and Bulla, L. A., Jr. (2006) A mechanism of cell death involving an adenylyl cyclase/PKA signaling pathway is induced by the Cry1Ab toxin of *Bacillus thuringiensis*. *Proc. Natl. Acad. Sci. U.S.A. 103*, 9897–9902.
13. Burton, S. L., Ellar, D. J., Li, J., and Derbyshire, D. J. (1999) N-acetylgalactosamine on the putative insect receptor aminopeptidase N is recognised by a site on the domain III lectin-like fold of a *Bacillus thuringiensis* insecticidal toxin. *J. Mol. Biol. 287*, 1011–1022.
14. Luo, K., Sangadala, S., Masson, L., Mazza, A., Brousseau, R., and Adang, M. J. (1997) The *Heliothis virescens* 170-kDa aminopeptidase functions as "Receptor A" by mediating specific *Bacillus thuringiensis* Cry1A δ-endotoxin binding and pore formation. *Insect Biochem. Mol. Biol. 27*, 735–743.
15. Valaitis, A. P., Mazza, A., Brousseau, R., and Masson, L. (1997) Interaction analyses of *Bacillus thuringiensis* Cry1A toxins with two aminopeptidases from gypsy moth midgut brush border membranes. *Insect Biochem. Mol. Biol. 27*, 529–539.
16. Nakanishi, K., Yaoi, K., Nagino, Y., Hara, H., Kitami, M., Atsumi, S., Miura, N., and Sato, R. (2002) Aminopeptidase N isoforms from the midgut of *Bombyx mori* and *Plutella xylostella*—their classification and the factors that determine their binding specificity to *Bacillus thuringiensis* Cry1A toxin. *FEBS Lett. 519*, 215–220.
17. Masson, L., Lu, Y. J., Mazza, A., Brousseau, R., and Adang, M. J. (1995) The CryIA(c) receptor purified from *Manduca sexta* displays multiple specificities. *J. Biol. Chem. 270*, 20309–20315.
18. Yaoi, K., Nakanishi, K., Kadotani, T., Imamura, M., Koizumi, N., Iwahana, H., and Sato, R. (1999) *Bacillus thuringiensis* Cry1Aa toxin-binding region of *Bombyx mori* aminopeptidase N. *FEBS Lett. 463*, 221–224.
19. Nakanishi, K., Yaoi, K., Shimada, N., Kadotani, T., and Sato, R. (1999) *Bacillus thuringiensis* insecticidal Cry1Aa toxin binds to a highly conserved region of aminopeptidase N in the host insect leading to its evolutionary success. *Biochim. Biophys. Acta 1432*, 57–63.
20. Chen, J., Aimanova, K. G., Pan, S., and Gill, S. S. (2009) Identification and characterization of *Aedes aegypti* aminopeptidase N as a putative receptor of *Bacillus thuringiensis* Cry11A toxin. *Insect Biochem. Mol. Biol. 39*, 688–696.
21. Zhang, R., Hua, G., Andacht, T. M., and Adang, M. J. (2008) A 106-kDa aminopeptidase is a putative receptor for *Bacillus thuringiensis* Cry11Ba toxin in the mosquito *Anopheles gambiae*. *Biochemistry 47*, 11263–11272.
22. Chen, J., Hua, G., Jurat-Fuentes, J. L., Abdullah, M. A., and Adang, M. J. (2007) Synergism of *Bacillus thuringiensis* toxins by a fragment of a toxin-binding cadherin. *Proc. Natl. Acad. Sci. U.S.A. 104*, 13901–13906.
23. Park, Y., Abdullah, M. A., Taylor, M. D., Rahman, K., and Adang, M. J. (2009) Enhancement of *Bacillus thuringiensis* Cry3Aa and Cry3Bb toxicities to Coleopteran larvae by a toxin-binding fragment of an insect cadherin. *Appl. Environ. Microbiol. 75*, 3086–3092.
24. Park, Y., Hua, G., Abdullah, M. A. F., Rahman, K., and Adang, M. J. (2009) Cadherin fragments from *Anopheles gambiae* synergize *Bacillus thuringiensis* Cry4Ba's toxicity against *Aedes aegypti* larvae. *Appl. Environ. Microbiol. 75*, 7280–7282.
25. Lobley, A., Whitmore, L., and Wallace, B. A. (2002) DICHROWEB: an interactive website for the analysis of protein secondary structure from circular dichroism spectra. *Bioinformatics 18*, 211–212.
26. Whitmore, L., and Wallace, B. A. (2004) DICHROWEB, an online server for protein secondary structure analyses from circular dichroism spectroscopic data. *Nucleic Acids Res. 32*, W668–W673.
27. Whitmore, L., and Wallace, B. A. (2008) Protein secondary structure analyses from circular dichroism spectroscopy: methods and reference databases. *Biopolymers 89*, 392–400.
28. Sreerema, N., Venyaminov, S. Y., and Woody, R. W. (1999) Estimation of the number of helical and strand segments in proteins using CD spectroscopy. *Protein Sci. 8*, 370–380.
29. Hua, G., Jurat-Fuentes, J. L., and Adang, M. J. (2004) Bt-R_{1a} extracellular cadherin repeat 12 mediates *Bacillus thuringiensis* Cry1Ab binding and cytotoxicity. *J. Biol. Chem. 279*, 28051–28056.
30. Silva-Filha, M. H., Nielsen-Leroux, C., and Charles, J. F. (1997) Binding kinetics of *Bacillus sphaericus* binary toxin to midgut brush-border membranes of *Anopheles* and *Culex* sp. mosquito larvae. *Eur. J. Biochem. 247*, 754–761.
31. Bradford, M. (1976) A rapid and sensitive method for the quantitation of microgram quantities of protein utilizing the principle of protein-dye binding. *Anal. Biochem. 72*, 248–254.
32. Garczynski, S. F., and Adang, M. J. (1995) *Bacillus thuringiensis* CryIA(c) δ-endotoxin binding aminopeptidase in the *Manduca sexta* midgut has a glycosyl-phosphatidylinositol anchor. *Insect Biochem. Mol. Biol. 25*, 409–415.
33. Garczynski, S. F., Crim, J. W., and Adang, M. J. (1991) Identification of putative insect brush border membrane-binding molecules specific to *Bacillus thuringiensis* delta-endotoxin by protein blot analysis. *Appl. Environ. Microbiol. 57*, 2816–2820.
34. Pacheco, S., Gómez, I., Gill, S. S., Bravo, A., and Soberón, M. (2009) Enhancement of insecticidal activity of *Bacillus thuringiensis* Cry1A toxins by fragments of a toxin-binding cadherin correlates with oligomer formation. *Peptides 30*, 583–588.
35. Soberón, M., Pardo-Lopez, L., Lopez, I., Gómez, I., Tabashnik, B. E., and Bravo, A. (2007) Engineering modified Bt toxins to counter insect resistance. *Science 318*, 1640–1642.
36. Peng, D., Xu, X., Ye, W., Yu, Z., and Sun, M. (2010) *Helicoverpa armigera* cadherin fragment enhances Cry1Ac insecticidal activity by facilitating toxin-oligomer formation. *Appl. Microbiol. Biotechnol. 85*, 1033–1040.
37. Pacheco, S., Gómez, I., Arenas, I., Saab-Rincon, G., Rodríguez-Almazán, C., Gill, S. S., Bravo, A., and Soberón, M. (2009) Domain II loop 3 of *Bacillus thuringiensis* Cry1Ab toxin is involved in a "ping pong" binding mechanism with *Manduca sexta* aminopeptidase-N and cadherin receptors. *J. Biol. Chem. 284*, 32750–32757.
38. Jenkins, J. L., Lee, M. K., Valaitis, A. P., Curtiss, A., and Dean, D. H. (2000) Bivalent sequential binding model of a *Bacillus thuringiensis* toxin to gypsy moth aminopeptidase N receptor. *J. Biol. Chem. 275*, 14423–14431.